Comparison of H_∞ with QFT applied to an Altitude Command Tracker for an UAV

J. López, R. Dormido, J. P. Gómez, S. Dormido, J. M. Díaz

***Abstract*— The main objective of this paper is to design and compare two altitude command tracker controllers for an UAV using H∞ and QFT techniques. Both methods require the use of specialized software tools. The different stages of QFT methodology have been done with help of software tool QFTIT (Quantitative Feedback Theory Interactive Tool). This is a free software tool that is characterized by its easy of use and interactive nature. QFT's standing as a viable control design method that can be applied to practical problems and produce implementable results. Tests with realistically large control inputs are use to validate and compare both designs.**

I. Introduction

THERE is a considerable and great interest in using unmanned vehicles to perform a multitude of tasks [1]-[2]. UAVs already provide clear opportunity to reduce the risk of life threatening missions that might otherwise be performed by human-piloted craft.

Nevertheless, the design of control systems for UAVs is clearly a complex task. The aircraft's response to control inputs depends heavily on the parameter uncertainties of the plant. For instance, the variations in the center of gravity or the time varying dependence of the mass affect to the control response. Hence, it is necessary the use of robust design methods with satisfactory performance over a specified range of plant parameter variations [3]-[5].

In [6] an autonomous flight control strategy is presented. The control task of that strategy is divided into two parts, a robust inner-loop controller that is designed to achieve stability and robustness to expected parameter uncertainty; and an outer-loop for tracking reference performace. A controller designed with the H∞ technique for the inner loop was presented in that paper.

In this paper two different altitude command tracker control strategies for the outer loop capable of high-performance tracking of a given flight trajectory in presence of parameter uncertainty have been compared. The first is an H_∞ approach, the second a QFT design. Advantages and disadvantages of both designs are described.

In Section II of this paper the modeling and identification assumptions are outlined. Section III presents the statement of the control problem. Section IV and V detail the H∞ and QFT designs. Validation is presented in Section VI. Concluding remarks are made in Section VII.

II. Modeling and Identification

The UAV is a 1/3 scaled down model of a Diamond Katana DA-20 shown in Fig. 1.

Fig. 1. KUAV scale model.

The main characteristics of the aircraft are:

--Span 3.9 m.

--Wing surface 1.47 square meters.

--Mean aerodynamic chord 0.39 m.

Manuscript received October 13, 2006. This work was supported in part by the Spanish Ministry of Industry under project SISCANT (Reference number FIT-330101-2004-13) and SISCANT II (Reference number FIT-330100-2005-129).

J. López is with Dynamic Systems Research Group, Universidad Politécnica de Madrid.

R. Dormido is with Department of Informática y Automática, Universidad Nacional de Educación a Distancia (UNED) (corresponding author to provide phone: +34-91-3987192; fax: +34-91-3987690; e-mail: raquel@dia.uned.es)

J. P. Gómez is head of Dynamic Systems Research Group, Universidad Politécnica de Madrid (e-mail: jgomez@euita.upm.es).

S. Dormido is with Department of Informática y Automática, Universidad Nacional de Educación a Distancia (UNED) (e-mail: sdormido@dia.uned.es)

J. M. Díaz is with Department of Informática y Automática, Universidad Nacional de Educación a Distancia (UNED) (e-mail: josema@dia.uned.es)

--Mass 18-30 kg.

--Cruise velocity 130 km/h.

--Maximum velocity 200 km/h.

--Engine power 8 HP.

--Centre of gravity between 15 and 31% of mean aerodynamic chord.

Aircraft dynamics are described by a set of nonlinear differential equations [7]. The resulting model is decribed by a thirteen state order model [15]. The main parameters of the aircraft are determined by a complete identification flight set through the full envelope. See [8]-[18] for details.

In order to design an altitude command tracker using linear design methods, it is necessary to obtain a state space linear model of the form:

$$\begin{aligned} \dot{x} &= Ax + Bu \\ y &= Cx + Du \end{aligned} \tag{1}$$

where the state, output and control vectors are respectively:

$$\begin{aligned} x &= \left[V_T \;\; \alpha \;\; \beta \;\; \phi \;\; \theta \;\; \psi \;\; P \;\; Q \;\; R \;\; p_N \;\; p_E \;\; h \;\; pow\right]^T \\ y &= \left[a_x \;\; a_y \;\; a_z \;\; P \;\; Q \;\; R \;\; lon \;\; lat \;\; h \;\; \dot{p}_N \;\; \dot{p}_E \;\; \dot{h}\right]^T \\ u &= \left[\delta_{tl} \;\; \delta_e \;\; \delta_a \;\; \delta_r\right]^T \end{aligned} \tag{2}$$

The state vector components are: true airspeed (V_T), angle of attack (α), sideslip angle (β), roll angle (ϕ), pitch angle (θ), yaw angle (ψ), roll rate (P), pitch rate (Q), yaw rate (R), north position (p_N), east position (P_E), altitude (h) and power (pow).

The output vector is formed by: x-component of acceleration (a_x), y-component of acceleration (a_y), z-component of acceleration (a_z), roll rate (P), pitch rate (Q), yaw rate (R), longitude (lon), latitude (lat), altitude (h), north position derivative ($\dot{p}_N$), east position derivative ($\dot{p}_E$) and altitude derivative ($\dot{h}$).

The control vector is defined by: throttle (δ_{tl}) , elevator (δ_e), aileron (δ_a) and rudder (δ_r).

The dynamics are linearized about a representative flight condition. This nominal condition is: $V_T = 30\,m/s$, centre of gravity position=25% of mean aerodynamic chord, ϕ=0 rad, $\psi = 0$ rad, $R = 0$ rad, $P = 0$ rad, $\theta = 0$ rad, rate of climb = 0 rad and lateral acceleration = 0 rad.

III. Statement of the Control Problem

The objective is the design of a controller capable of tracking altitude commands. Stability of the aircraft, minimal overshoot and a reasonably long settling time are important constrains. Translated into physical design goals, the controller must perform the following specifications:

--The controlled system should be able to track altitude commands with rise time tr < 5 s.

--Settling time ts < 20 s.

--The overshoot (Mp) in the response to unit steps at altitudes above 300 m should be Mp < 5%. At lower altitudes Mp may increase to 30% in order to obtain higher tracking performance.

Landing operation is not an easy task. In the final phase of flight it is necessary to be able to accurately maintain the desired rate of descent (the so called glide path) of the aircraft. In this sense, specifications impose that the vertical deviation from the desired flight path should not exceed that given in the Fig. 2.

A possible strategy to design an UAV controller that fulfills the specifications consists in dividing the control architecture in two parts: an inner-loop controller to achieve stability and robustness to expected parameter uncertainty; and an outer-loop for tracking reference performaces. This architecture is based in that proposed by Tucker and Walker [9].

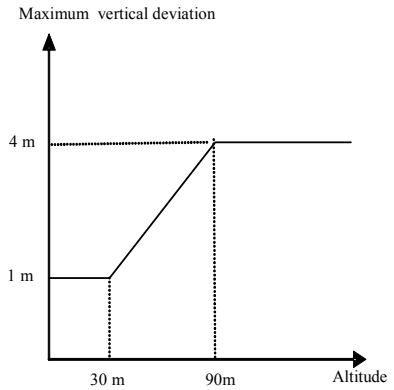

Fig. 2. Specifications for approach glide path.

In Fig. 3 the complete control architecture is shown. The inputs to the inner-loop controller are vertical speed, airspeed and roll angle. This controller was designed in [6] using the H_∞ technique. The controller designed guarantees the stability and follows an ideal model, the so called matching model (M).

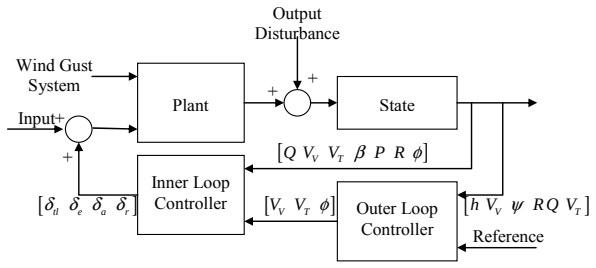

Fig. 3. Control architecture.

The matching model M, which defines the behaviour of the vertical speed, the true speed and the heading angle consists of the following three second order systems:

$$M = \begin{bmatrix} \frac{4^2}{s^2+2\cdot 4s+4^2} & 0 & 0 \\ 0 & \frac{1.5^2}{s^2+2\cdot 1.5s+1.5^2} & 0 \\ 0 & 0 & \frac{2.25^2}{s^2+2\cdot 2.25s+2.25^2} \end{bmatrix} \quad (3)$$

Two different controllers conforms the outer-loop: The height controller and the heading and lateral deviation controller.

In this paper the synthesis of the height tracking reference controller is performed using the H_∞ loop shaping technique [10] and also using a QFT design [11]. Then both designs are compared.

Fig. 4 shows the problem to be solved.

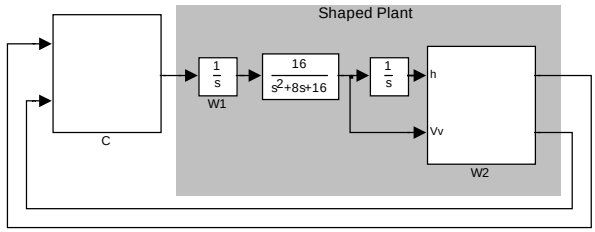

Fig. 4. Outer-loop altitude command tracker.

The structure of the controller is shown in Fig. 5.

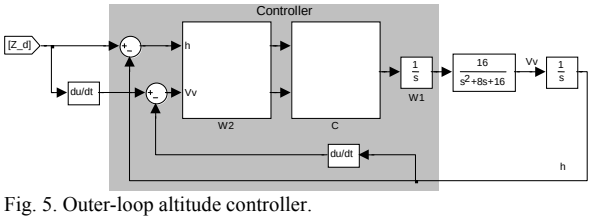

Fig. 5. Outer-loop altitude controller.

The inputs to the outer-loop controller are altitude reference, vertical velocity reference and heading angle reference.

The plant in Fig. 4 is the desired vertical velocity model (see [6] for details) defined by the first element of the ideal model M, that is

$$\frac{4^2}{s^2+8s+4^2} \quad (4)$$

Different plant uncertainties can affect to the nominal system such as different configurations of the center of gravity and mass variation. To face the robustness problem, a set of possible plants are defined by means of an upper and lower limit to (4). This set is shown in Fig. 6.

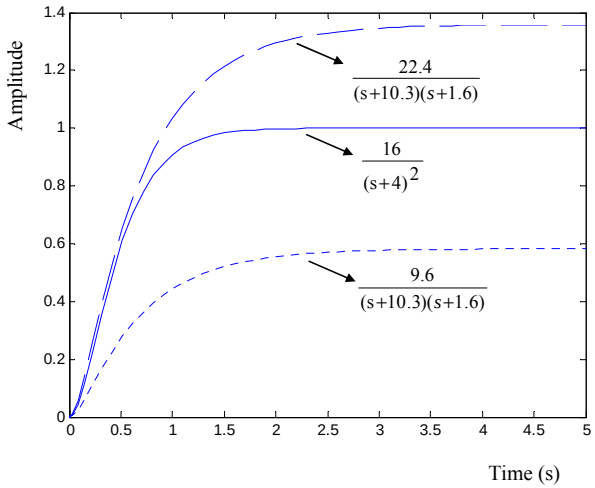

Fig. 6. Plant Uncertainty.

These bounds are calculated bounding the step responses behaviours of the system when changes occurs in parameters of the system such as a variation in the center of gravity or in the mass. It's important to note that plant uncertainty has been defined in a very conservative way.

IV. H_∞ DESIGN

The synthesis of the height tracking reference controller is performed using the well known H_∞ loop shaping technique [10]-[12].

This is a regulation problem where the variables to be controlled are the height and the vertical velocity. In this case the system is one input and two outputs. The scaled system model is shaped using pre and postcompensator weights of the form: $W_1 Plant W_2$

The precompensator (W_1) is selected as an integrator to boost the low frequency gain. This ensures zero steady-state tracking error and disturbance rejection. W_2 (the postcompensator) is chosen as a constant: diag[0.5, 0.88] to change the gain in a properly way. In this work weights have been selected using a trial and error method. Of couse, it should be interesting to study this selection to improve the controller performance.

The resulting sub-optimal robust stability margin is: γ = 3.18 and the controller order was 5. The design is usually considered successful if $\gamma < 4$ [4].

The controller obtained is showed in (5). It is a three inputs system (aircraft altitude, aircraft vertical velocity and commanded altitude) due to some algebraic transformations applied to calculate the commanded vertical velocity inside the controller ([6]).

$$A_C = \begin{bmatrix} 0 & 1.08 & 0.69 & 1.25 & 0.68 \\ 0 & -1.08 & -0.69 & -8.70 & -3.21 \\ 0 & 0.85 & -3 & -2.16 & -0.25 \\ 0 & 0 & 1.65 & -2.93 & -1.03 \\ 0 & 0 & 0 & -3.24 & -1.93 \end{bmatrix}$$

$$B_C = \begin{bmatrix} 0 & 0 & -9.55 \\ 1.86 & 4.64 & 28.28 \\ 0.17 & 0.50 & 2.04 \\ 0.75 & 1.83 & 6.61 \\ 1.42 & 2.75 & 9.83 \end{bmatrix} \qquad (5)$$

$$C_C = \begin{bmatrix} 1 & 0 & 0 & 0 & 0 \end{bmatrix}$$

$$D_C = \begin{bmatrix} 0 & 0 & 0 \end{bmatrix}$$

The compensated plant step and ramp response is showed in Fig. 7 and Fig. 8 respectively.

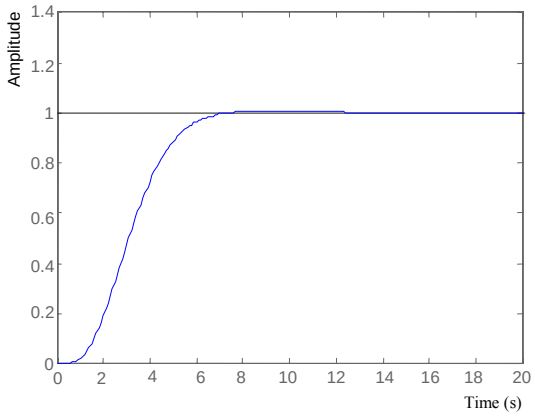

Fig. 7. Compensated plant step response.

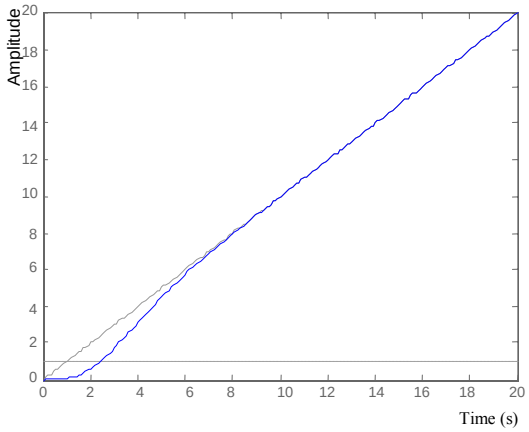

Fig. 8. Compensated plant ramp response.

V. QFTIT DESIGN

To solve this problem the free interactive software tool QFTIT (http://ctb.dia.uned.es/asig/qftit/) is chosen. To face the problem using QFTIT first it's necessary to divide the problem into two independent SISO problems. One of them controls the height and the other controls the vertical velocity. Then, using QFTIT it is possible to implement the different QFT stages in order to design a robust monovariable controller [13]-[14].

When the controllers are working together an interaction is produced between them. To obtain the desired behavior a trial and error iterative process was accomplished until the two controllers are correctly tuned.

The stages required in a QFT controller design are four: Template computation, Specifications, Loop-shaping and Validation [14]. The realization of each of the QFT stages

using QFTIT for solving the height and the vertical velocity SISO controllers are described below.

A. *The height controller*

As described in Section III, (4) defines the desired vertical velocity behaviour. If (4) is integrated then an expression which defines the heigh behaviour is obtained. In order to study robustness properties, it can be defined a family of plants P defined as a transfer function with parametric uncertainties in its coefficients of the form:

$$\mathrm{P}=\begin{cases} P(s)=\dfrac{k}{s(s+a)^2} \\ k\in[9.6,22.4] \\ a\in[1.6,10.3] \end{cases} \tag{6}$$

where the nominal plan can be expressed as

$$P_0=\frac{16}{s(s+4)^2} \tag{7}$$

The problem to solve is to design a controller *C*, so that for all $P\in \mathrm{P}$ the system is stable (robust stability) and for all disturbance $d\in\Delta$ disturbance rejection is obtained. The system considered it is shown in Fig. 9

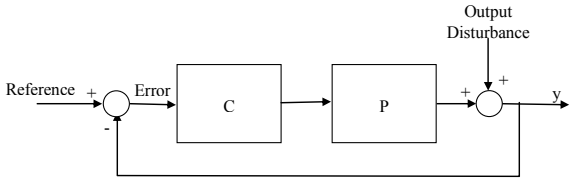

Fig. 9. SISO regulation structure.

In the first step of the design, the plant uncertainty and the frequencies set are introduced in QFTIT using its drag and drop characteristics.

From the study of the desired crossover frequency it can be deduced that a possible set of trial frequencies is:

$$\Omega=[0.0001,0.001,0.01,0.1,1,5,10,100] \tag{8}$$

QFTIT automatically computes the magnitude and phase of the family of plants in each frequency corresponding to a set of points in the Nichols diagram. These regions are called templates. Fig. 10 shows the templates computation window of QFTIT.

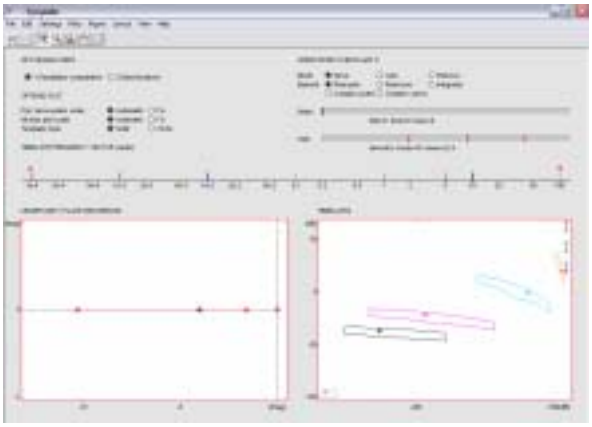

Fig. 10. QFTIT: Templates computation for height controller.

In this window can be distinguished different areas. The template frequency vector is located in the central part of the window and it is used to configure the value of the frequency vector Ω (10). In the left lower part of the window using a map of poles and zeros the uncertainty plant description is configured. In the right lower part of the window a Nichols diagram with the templates and its nominal value is shown.

Second stage implies to configure the specifications that the design must fulfil. Three specifications are taken into account in this problem: robust stability, disturbance rejection and control effort. They are implemented in QFTIT through the conditions given in (9).

$$\begin{aligned} &\textit{Robust stability}: \left|\frac{P\cdot k}{1+PC}\right|<W_{s1} \\ &\textit{Disturbance rejection at plant output}: \left|\frac{1}{1+PC}\right|<W_{s2} \\ &\textit{Control effort}: \left|\frac{k}{1+PC}\right|<W_{s3} \end{aligned} \tag{9}$$

For each specification it must be selected the value of its W_{si}, i=1,2,3. The frequencies under which each specification must be verified also have to be selected (see Table I).

TABLE I
PECIFICATIONS LIMITS

Type	Limit Value	Frequencies
W_{s1}	1.01	10, 100
W_{s2}	0.4	1e-4, 1e-3, 1e-2
W_{s4}	0.2	10, 100

Finally, the loop-shaping is accomplished (see Fig. 11).

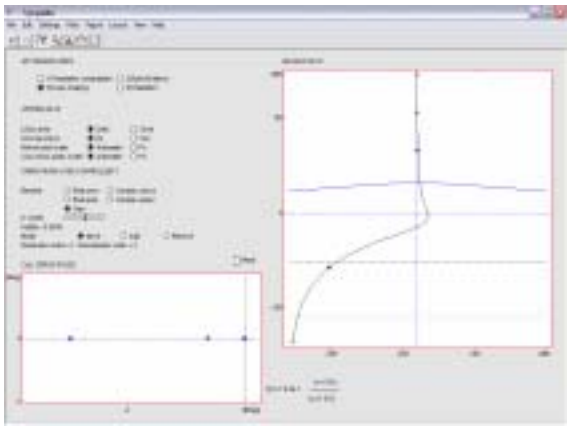

Fig. 11. QFTIT: Loop shaping for height controller.

QFTIT allows adding dynamically poles and zeros and dragging them over Nichols chart (located on the right of the window) until the specifications boundaries are satisfied. In our particular problem an integrator is added to improve low frequency performance. Fig. 11 displays the aspect of the QFTIT window after loop-shaping stage.

The expression of the designed controller is

$$C = 0.94\frac{s+0.6}{s(s+30)} \tag{10}$$

B. The vertical velocity controller

In this case the family of plants is given by

$$\mathrm{P} = \begin{cases} P(s) = \dfrac{k}{(s+a)^2} \\ k \in [9.6, 22.4] \\ a \in [1.6, 10.3] \end{cases} \tag{11}$$

The nominal values are $k_{nom} = 16$ and $a_{nom} = 4$.

In the design of the vertical velocity controller, the frequencie set is given by (8). The specifications that the design should satysfy are presented in (9). The values of the frequencies under which each specification must be satisfied are the same as the calculated for the height controller (see Table I).

The templates computation is showed in Fig. 12.

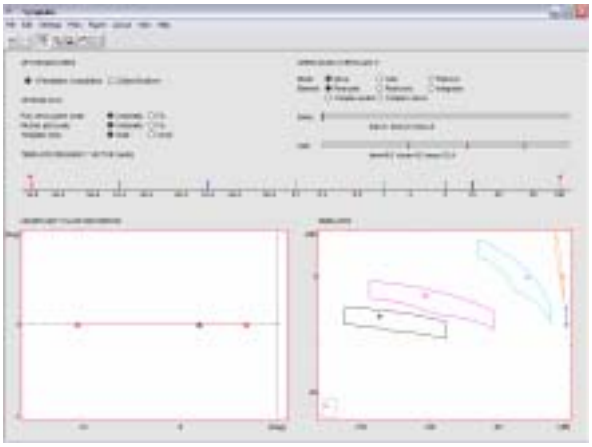

Fig. 12. QFTIT: Templates computation for vertical velocity controller.

Fig. 13 displays the shaped plant obtained in the design. The controller obtained is

$$C = 0.94\frac{s+0.6}{s(s+30)} \tag{12}$$

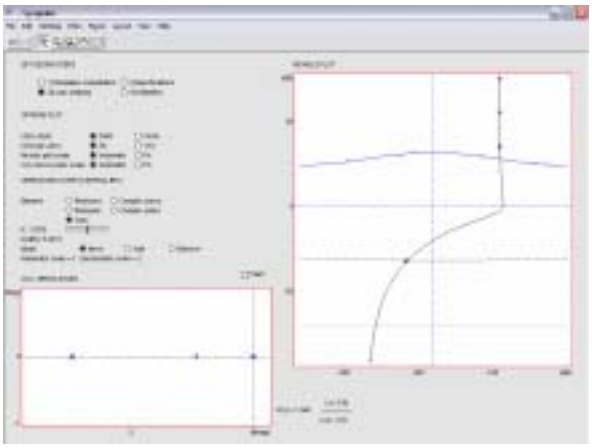

Fig. 13. QFTIT: Loop shaping for vertical velocity controller.

The two controllers joined (10) and (12) are showed in Fig. 14. C_h is the height controller and C_v corresponds to the vertical velocity controller.

It's important to note that in order to obtain a reasonably performance it is necessary an iterative and sometimes tedious trial and error process.

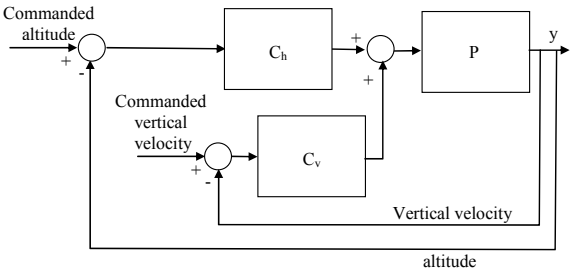

Fig. 14. QFT controllers configuration.

VI. CONTROLLER TESTING

In order to compare and validate the controllers designed, a set of test cases have been developed. Below, an experience corresponding to 30 m altitude step response is shown for the two controllers developed. These simulations allow to compare the behavior of the aircraft using both designs. It will be easy to check that during this maneuver it can be seen how the elevator works to change the attitude of the aircraft to nose up and then the throttle acts to maintain the velocity. Later the throttle is released while the elevator nose down the aircraft progressively.

Fig. 15 represents the altitude response. It presents a very little overshoot, rise time over 5 seconds and settling time around 14 seconds for both controllers. The QFT controller behavior is smooth, however, the H_∞ controller presents around second 3, a little change in vertical velocity.

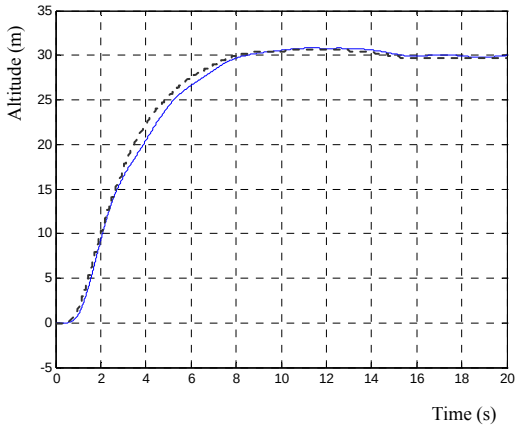

Fig. 15. 30 m altitude step response with H_∞ (solid) and QFT (dashed) controller.

As can be notice from Fig. 16, throttle doesn't reach its saturation value. With the H_∞ controller the response is oscillating until stabilization is reached at trim position (18 seconds). QFT controller doesn't present oscillations and comes back quickly to trim condition (about 8 seconds).

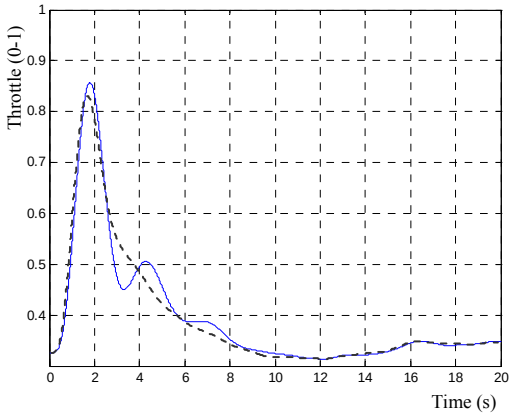

Fig. 16. Throttle behavior during a 30 m altitude step response with H_∞ (solid) and QFT (dashed) controller.

Fig. 17 shows how the elevator doesn't reach its saturation value.

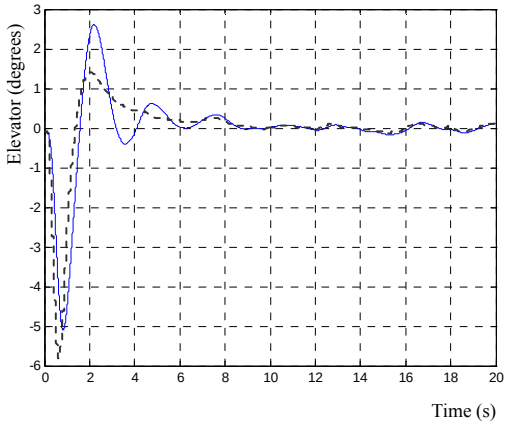

Fig. 17. Elevator behavior during a 30 m altitude step response with H_∞ (solid) and QFT (dashed) controller.

The maximum and minimum values are similar in both designs, but QFT controller doesn't present oscillations and reach the equilibrium value around 6 seconds.

VII. CONCLUSIONS

H_∞ and robust QFT control system design methods are used to design an altitude command tracker controller.

The H_∞ and the QFT controllers designed are compared. The effectiveness of each method through the analysis of the stability and performance of the controller to an uncertain aircraft it is analyzed.

It is shown that both controllers guarantee the robust stability and nominal performance requirements. Moreover, both designs attenuate high frequency noise due to sensors supplying suitable control signals. Test experiences show that

QFT design gives a smoother performance and a control effort sligtly less than the one obtained with the H_∞ controller. As it was expected, QFT leads to lower order controller (order 2) with comparable results to that obtained with H_∞ (order 5).

It is important to notice that the speed at which a QFT design can be performed is heavily influenced by the experience of the user, H_∞ is less user dependent. Nevertheless, specialised software tools reduce the required skill and experience for loop shaping in QFT. In this sense, the use of QFTIT makes easy the different stages of QFT. This free software tool allows designers change interactively the parameters involved in the design.

REFERENCES

[1] Office of the Secratry od Defense. "Unmanned aircraft systems roadmap 2005-2030". Technical report, United States Departmente of Defense, 2005.

[2] Wegener S, "UAV over-the–horizon disaster management demonstration projects". NASA Ames Research Center, 2001.

[3] R. A. Hyde, "H∞ Aerospace Control Design: A VSTOL Flight Application". Berlin; New York: Springer, 1995.

[4] B. M. Chen. "H∞ control and is applications". London; New York: Springer, 1998.

[5] R. J. Adams, "Robust Multivariable Flight Control". London; New York: Springer Verlag: 1994.

[6] Gómez, P., López, J., Monteagudo, A., "Robust Controllers Design Strategies for Unmanned Air Vehicles: H∞". *ICAS 2006.*

[7] Stevens, B. L., Lewis, F. L., "Aircraft Control and Simulation". Wiley-Interscience. 1992.

[8] López, J., Dormido, R., "Diseño de un Sistema de Control para un UAV Comercial". Internal Report DIA 330-1.

[9] Tucker, M. R., Walker, D. J., "RCAM Design Challenge Presentation Document: An H infinite Approach". GARTEUR TP-088-21. 1997.

[10] McFarlane, Glover, "A loopshaping design procedure using H∞ synthesis", *IEEE Transactions on Automatic Control vol. 37 pp-759-769, 1992.*

[11] Horowitz, I. M., "Synthesis of feedback systems". New York: Academic Press, 1963.

[12] Skogestad S., Postlethwaite, I., "Multivariable Feedback Control". Wiley. 1996.

[13] Díaz, J. M., Dormido, S., Aranda, J., "Interactive computer-aided control design using quantitative feedback theory: the problem of vertical movement stabilization on a high-speed ferry". *International Journal of Control. Vol 78, No 11, 20 July 2005, 813-825.*

[14] Houpis, C. H., Rasmussen, S. J., Garcia, M., "QFT: Fundamentals and Applications". Wiley. 2005.

[15] Lambrechts, P., Bennani, S., Looye, G, Helmersson, A. et alter. "Robust Flight Control Design Challenge Problem Formulation and Manual: RCAM". GARTEUR. 1997.

[16] Ogata, K. "Ingeniería de Control Moderna". Prentice Hall. 1993.

[17] Ward, D. G., Sharma, M., Richards, N. D. "Intelligent Control of Unmanned Air Vehicles: Program Summary and Representative Results". AIAA. 2003.

[18] López, J., Gómez, I., Gómez, J.P., Dormido, R.. "Development of an UAV Full envelope Flight Control System Using H∞ Techniques". EURO UAV 2006.